Broken pairs in the interacting boson model: Projection of spurious states

Cacciamani, S.; Bonsignori, G.; Iachello, F.; Vretenar, Dario

Broken pairs in the interacting boson model: Projection of spurious states

S. Cacciamani and G. Bonsignori
INFN Sez. di Bologna and Department of Physics, University of Bologna, Bologna, Italy

F. Iachello
Center for Theoretical Physics, Yale University, New Haven, Connecticut 06511

D. Vretenar
Physics Department, Faculty of Science, University of Zagreb, 41000 Zagreb, Croatia
(Received 23 June 1995)

The interacting boson model is extended by the inclusion of selective noncollective fermion states through the successive breaking of the correlated S and D pairs (s and d bosons). High angular momentum states are generated in this way, and their structure described by the coupling between fermions in broken pairs and the boson core. The model space of bosons and broken pairs contains also unphysical states that are generated automatically when fermions couple to angular momenta $J_F=0$ and 2. A procedure is derived for the projection of spurious components from bases that contain one fermion pair. Spurious states are identified and an algorithm for their projection is constructed. The model is applied to the description of states in the spherical nucleus ^{116}Sn, and the weakly deformed nucleus ^{82}Sr. Calculated spectra and transition probabilities are compared with experimental data. It is found that projection of spurious states from the model space is essential for a description of excited states with low angular momenta above the yrast, while it is less important for high-spin states close to the yrast line.

PACS number(s): 21.60.Fw, 21.60.Ev, 27.50+e, 27.60.+j

I. INTRODUCTION

Models of nuclear structure that are based on the interacting boson approximation (IBA) [1], provide a unified framework for the description of medium heavy and heavy nuclei. Over the years numerous extensions of the original interacting boson model (IBM-1) [2] have been investigated [1,3]. Among these, there are models that extend the IBM to the physics of high-spin states. To apply the model to the description of high-spin states in nuclei ($10\hbar \leqslant J \leqslant 30\hbar$), one has to go beyond the interacting boson approximation and extend the model space by including, in addition to bosons, part of the original shell model space for valence nucleons. This is done by breaking the correlated S and D pairs (s and d bosons) to form selective noncollective fermion pairs. High-spin states are described in terms of broken pairs.

Several extensions of the IBM have been reported that include two-fermion states (one broken pair) in addition to bosons. In one of the first papers [4] Gelberg and Zemel used an empirical model to incorporate two-particle states in an SU(3) boson basis and investigated backbending phenomena. Faessler *et al.* [5,6] have proposed a semimicroscopic model, based on the IBM-1, for the inclusion of two-quasiparticle states in a boson basis. The model has been successfully applied to the description of high-spin states in Hg, Ba, and Ce isotopes. This approach was also used to study yrast high-spin states in odd-mass Hg isotopes by extending the IBFM to include three-quasiparticle states [7]. Yoshida, Arima, and Otsuka [8] extended the proton-neutron IBM (IBM-2) to include states with two fermions. The model has been used to analyze high-spin states in Ba and Ce [8], Ge [9], and Dy [10] isotopes. Zemel and Dobes [11] have used the IBM-2 plus two-quasiparticle model to describe properties of low-spin states in Po and Rn isotopes. More recently, using an interacting boson-plus-fermion pair model, Chuu, Hsieh, and Chiang have investigated in a series of papers the structure of high-spin states in Pt [12], Dy [13], Er [14], Ge [15], and U [16] isotopes. In Refs. [17–26] we have further extended the IBM to include two- and four-fermion noncollective states (one and two broken pairs), and applied the model in the description of high-spin states in the Hg [18,22,26], Sr-Zr [20,23,24], and Nd-Sm [25] regions.

The model that we have used is based on the simplest version of the interacting boson (fermion) model: IBM-1/IBFM-1 [2,27]. The boson space consists of s and d bosons, with no distinction between protons and neutrons. The bosons represent collective fermion pair states (correlated S and D pairs) that approximate the valence nucleons pairs. To generate high-spin states, the model allows one or two bosons to be destroyed and form noncollective pairs, represented by two- and four-quasiparticle states that couple to the boson core. The model space for an even-even nucleus with $2N$ valence nucleons can be written as

$$\begin{aligned}|2N\text{fermions}\rangle = &|(N)\text{bosons}\rangle \\ &\oplus|(N-1)\text{bosons}\otimes 1\text{broken pair}\rangle \\ &\oplus|(N-2)\text{bosons}\otimes 2\text{broken pairs}\rangle \\ &\oplus \ldots .\end{aligned}$$

Although generally fermions in broken pairs occupy all the valence single-particle orbitals from which the bosons have been mapped, for the description of high-spin states close to

the yrast line the most important are the unique parity orbitals ($g\frac{9}{2}$, $h\frac{11}{2}$, $i\frac{13}{2}$). The Coriolis antipairing effect is much more pronounced for states with high single-particle angular momentum. For low angular momenta j, the Coriolis force is weak and unable to break pairs.

The model space of bosons and broken pairs contains also unphysical states. By allowing the fermions in broken pairs to couple to angular momenta $J_F=0$ and 2, spurious states are introduced in the model, i.e., the basis does not strictly obey the Pauli principle. Particular linear combinations of fermion pairs are equivalent to the correlated S or D pairs (s or d bosons). Projection of the spurious components from the model space necessitates that all valence fermion orbitals are included in the basis, making it thus prohibitively large for more than one broken pair. The procedure consists in constructing the s and d bosons microscopically in the basis of valence fermion orbitals, and removing these linear combinations from the basis of broken pairs. Projection of spurious states was not included in models that extended the IBM with fermion pairs. In most versions, the $J_F=0$ and 2 fermion pairs simply were not included in the model space. In this way many physical states are also excluded from the basis. In Refs. [20–25] we have applied the model with one and two broken pairs to transitional nuclei. Fermion pairs with $J_F=0$ and 2 were kept in the basis. The justification was that the percentage of these components, and then the percentage of spurious components, in the wave functions of states close to the yrast line is negligible. However, even in this case the presence of spurious states can have an indirect effect on the strength of the mixing interaction in the region of band crossing.

In this paper we derive a procedure for projection of spurious components from bases that contain one fermion pair. This paper is organized as follows. In Sec. II we give a short outline of the model. Spurious states are identified and an algorithm for their projection is described in Sec. III. In Sec. IV we apply the model to the spherical nucleus ^{116}Sn. The IBM alone cannot describe the density of low-lying states in this nucleus; including explicit fermion degrees of freedom (broken pair), improves the results. In this case we find that it is very important to project spurious states from the fermion basis. In Sec. V we describe the structure of states and transitions close to the yrast line in the weakly deformed nucleus ^{82}Sr. According to our previous calculations in this region [20,23,24], projection of spurious states should not have a significant effect on the results.

II. THE MODEL

An even-even nucleus with $2N$ valence nucleons is described as a system of N interacting bosons. The model allows one boson to be destroyed and form a noncollective fermion pair. The structure of the model space is

$$\mathscr{M}\rightarrow|(N)\text{bosons}\rangle\oplus|(N-1)\text{bosons}\otimes 1\text{broken pair}\rangle. \quad (2.1)$$

The model Hamiltonian contains boson terms, fermion terms, and boson-fermion interactions

$$H=H_B+H_F+V_{BF}+V_{\text{mix}}. \quad (2.2)$$

H_B is the boson Hamiltonian of IBM-1 [1]

$$H_B=\epsilon\hat{n}_d+\sum_{L=0,2,4}\frac{1}{2}\sqrt{2L+1}c_L[(d^\dagger\times d^\dagger)^{(L)}\times(\tilde{d}\times\tilde{d})^{(L)}]^{(0)}$$
$$+\frac{1}{\sqrt{2}}v_2\{[(d^\dagger\times d^\dagger)^{(2)}\times(\tilde{d}\times s)^{(2)}]^{(0)}+\text{H.c.}\}$$
$$+\frac{1}{2}v_0\{[(d^\dagger\times d^\dagger)^{(0)}\times(s\times s)^{(0)}]^{(0)}+\text{H.c.}\}. \quad (2.3)$$

The fermion Hamiltonian H_F contains single-fermion energies and fermion-fermion interactions

$$H_F=\sum_\alpha E_\alpha a_\alpha^\dagger a_\alpha+\frac{1}{4}\sum_{abcd}\sum_{JM}V^J_{abcd}A^\dagger_{JM}(ab)A_{JM}(cd), \quad (2.4)$$

where the fermion pair operator is defined as

$$A^\dagger_{JM}(ab)=\frac{1}{\sqrt{1+\delta_{ab}}}[a_a^\dagger\times a_b^\dagger]^{(J)}_M, \quad (2.5)$$

and the matrix elements of the interaction are expressed through standard coefficients G^J and F^J of the shell model [28]

$$V^J_{abcd}=(u_au_bu_cu_d-v_av_bv_cv_d)G^J_{abcd}+4v_au_bv_cu_dF^J_{abcd}. \quad (2.6)$$

The first part of the interaction between the unpaired fermions and the boson core is the IBFM-1 boson-fermion interaction [3,27]

$$V_{BF}=V_{\text{dyn}}+V_{\text{exc}}+V_{\text{mon}}. \quad (2.7)$$

The quadrupole-quadrupole dynamical interaction is

$$V_{\text{dyn}}=\Gamma_0\sum_{j_1j_2}(u_{j_1}u_{j_2}-v_{j_1}v_{j_2})\langle j_1\|Y_2\|j_2\rangle([a^\dagger_{j_1}\times\tilde{a}_{j_2}]^{(2)}\cdot Q^B), \quad (2.8)$$

where the boson quadrupole operator is defined

$$Q^B=[s^\dagger\times\tilde{d}+d^\dagger\times\tilde{s}]^{(2)}+\chi[d^\dagger\times\tilde{d}]^{(2)}. \quad (2.9)$$

The exchange and monopole terms of the boson-fermion interaction are, respectively

$$V_{\rm exc}=-\Lambda_0 2\sqrt{5}\sum_{j_1 j_2 j_3}(2j_3+1)^{-\frac{1}{2}}(u_{j_1}v_{j_3}+v_{j_1}u_{j_3})\times(u_{j_2}v_{j_3}+v_{j_2}u_{j_3})\langle j_3\|Y_2\|j_1\rangle\langle j_3\|Y_2\|j_2\rangle\times:[(a^\dagger_{j_1}\times\tilde{d})^{(j_3)}\times(\tilde{a}_{j_2}\times d^\dagger)^{(j_3)}]^{(0)} \quad (2.10)$$

and

$$V_{\rm mon}=A_0\sqrt{5}\sum_j(2j+1)([a^\dagger_j\times\tilde{a}_j]^{(0)}\cdot[d^\dagger\times\tilde{d}]^{(0)}). \quad (2.11)$$

The fermion operators $a^\dagger$ and $\tilde{a}$ in (2.4)–(2.11) represent ideal fermions, in the sense that they commute with the boson operators $d^\dagger$ and $s^\dagger$. Since the bosons are mapped from correlated pairs of valence nucleons, commutation relations between boson operators and valence nucleon operators are nontrivial. With the introduction of ideal fermions, the bases generated by boson and fermion creation operators are orthogonal. In IBFM-1, the low-seniority approximation defines a boson image of the valence nucleon operator $c^\dagger_{jm}$ in terms of boson operators and ideal fermion operators $a^\dagger_{jm}$ [29,3]

$$c^\dagger_{jm}\rightarrow u_j a^\dagger_{jm}+\frac{\alpha_j}{\sqrt{\Omega}}(s^\dagger\tilde{a}_j)^{(j)}_m+u_j\frac{\sqrt{10}}{\hat{j}}\sum_{j'}\beta_{j'j}(d^\dagger\tilde{a}_{j'})^{(j)}_m-\frac{\alpha_j}{\sqrt{\Omega}}\frac{\sqrt{10}}{\hat{j}}s^\dagger\sum_{j'}\beta_{j'j}(\tilde{d}a^\dagger_{j'})^{(j)}_m, \quad (2.12)$$

where α_j and β_{ij} are related to structure constants of the s and d bosons, respectively.

The terms in the Hamiltonian H_B, H_F, and V_{BF} conserve the number of bosons and the number of fermions separately. In our model only the total number of nucleons is conserved, bosons can be destroyed and fermion pairs created, and vice versa. Using the same order of approximation as for V_{BF}, from the quadrupole boson-fermion interaction one derives the pair-breaking interaction $V_{\rm mix}$ [5], that mixes states with different number of fermions, conserving the total nucleon number only:

$$V_{\rm mix}=-U_0\left\{\sum_{j_1 j_2}u_{j_1}u_{j_2}(u_{j_1}v_{j_2}+u_{j_2}v_{j_1})\langle j_1\|Y_2\|j_2\rangle^2\frac{1}{\sqrt{2j_2+1}}([a^\dagger_{j_2}\times a^\dagger_{j_2}]^{(0)}\cdot s)+\text{H.c.}\right\}-U_2\left\{\sum_{j_1 j_2}(u_{j_1}v_{j_2}+u_{j_2}v_{j_1})\langle j_1\|Y_2\|j_2\rangle([a^\dagger_{j_1}\times a^\dagger_{j_2}]^{(2)}\cdot\tilde{d})+\text{H.c.}\right\}. \quad (2.13)$$

This is the lowest order contribution to a pair-breaking interaction. The first term represents the destruction of one s boson and the creation of a fermion pair, while in the second term a d boson is destroyed to create a pair of valence fermions.

III. THE MODEL SPACE AND SPURIOUS STATES

The model space contains bosons and fermion pair states. The fermion pairs should reside outside the S-D subspace in order to avoid double counting of states. This is not satisfied automatically, if the fermions are allowed to couple to angular momenta $J_F=0$ and 2. Instead, unphysical states are generated. In this section we identify the spurious states and derive a procedure for their projection from the model space. Technically, this procedure becomes quite complicated for more than one broken pair. Therefore we only consider the model space (2.1).

There are two types of states in the model space: boson states $|\Phi_B\rangle$ and boson-fermion states $|\Phi_{BF}\rangle$. For the boson states $|\Phi_B\rangle$ we take the IBM-1 model space without any modification

$$|\Phi_B\rangle=\frac{1}{\mathcal{N}_B}[(s^\dagger)^{N-n}\times(d^\dagger)^n_\nu]^{(J)}|0_B\rangle\otimes|0_F\rangle, \quad (3.1)$$

where the product of boson vacuum and fermion vacuum is indicated explicitly, $0\leq n\leq N$, and ν is an additional quantum number that specifies a state with n d bosons. $\mathcal{N}_B$ is the normalization constant. The vectors $|\Phi_{BF}\rangle$ contain one broken pair

$$|\Phi_{BF}\rangle=\frac{1}{\mathcal{N}_{BF}}[A^\dagger_{J_F}(ab)\times[(s^\dagger)^{N-1-n}\times(d^\dagger)^n_\nu]_{J_B}]^{(J)}|0_B\rangle\otimes|0_F\rangle, \quad (3.2)$$

where now $0\leq n\leq(N-1)$ and $A^\dagger$ is the creation operator of a pair of ideal fermions, defined in Eq. (2.5). We also define the analogous operator for shell-model valence nucleons, i.e., "real fermions"

$$C^\dagger_{JM}(ab)=\frac{1}{\sqrt{1+\delta_{ab}}}[c^\dagger_a\times c^\dagger_b]^{(J)}_M. \quad (3.3)$$

The collective operators $S^\dagger$ and $D^\dagger$ that create the correlated S and D pairs are, respectively,

$$S^\dagger=\sum_a\phi_a C^\dagger_{00}(aa)\rightarrow s^\dagger \quad (3.4)$$

and

$$D^\dagger_\mu=\sum_{ab}\chi_{ab}C^\dagger_{2\mu}(ab)\rightarrow d^\dagger_\mu, \quad (3.5)$$

where we also indicate the ''mapping'' to boson states. This correspondence is straightforward only in the case of one fermion pair [31]. The direct sum of vector spaces $|\Phi_B\rangle$ and $|\Phi_{BF}\rangle$ forms an orthonormal basis in which matrix elements of various operators are calculated. Without the mixing terms (2.13), the block off-diagonal matrix elements of the Hamiltonian vanish

$$\langle\Phi_{BF}|H|\Phi_B\rangle=\langle\Phi_B|H|\Phi_{BF}\rangle=0.$$

The boson space $|\Phi_B\rangle$ is completely decoupled from broken pairs. The low-lying states are those obtained in IBM-1. Only with the introduction of the mixing interaction (2.13) the two vector spaces couple, and one is able to describe physical effects as, for example, admixture of two-quasiparticle states in low-lying states, interaction between bands—backbending, alignment, etc.

In the process of destroying bosons and creating fermion pairs, i.e., in going back to the shell-model space of valence nucleons, unphysical states are introduced in the model space. With the term *noncollective fermion pair* we denote a two-fermion state which is not a vector in the *S*-*D* fermion space. If the ideal fermions that form the broken pair couple to angular momenta $J_F=0$ and 2, particular linear combinations of these configurations form states that are physically equivalent to boson states. The microscopic collective structure of bosons is reconstructed in terms of fermion pairs. This leads to double counting of states, since particular linear combinations of $|\Phi_{BF}\rangle$ states are equivalent to $|\Phi_B\rangle$ states. Fermions occupy twice the same orbitals and therefore violate the Pauli principle.

The linear combinations of vectors $|\Phi_{BF}\rangle$, that reproduce the microscopic structure of states $|\Phi_B\rangle$, present spurious states in the model space. We denote them by $|Z\rangle$. An example is the state that reconstructs the structure of the *s* boson

$$\begin{aligned}|Z\rangle&=\sum_a \tilde{\phi}_a[A_0^\dagger(aa)\times[(s^\dagger)^{N-1-n}\times(d^\dagger)^n]_J]^{(J)}|0_B\rangle\otimes|0_F\rangle\\&=\left[\left(\sum_a \tilde{\phi}_a A_0^\dagger(aa)\right)[(s^\dagger)^{N-1-n}\times(d^\dagger)^n]_J\right]^{(J)}|0_B\rangle\otimes|0_F\rangle.\end{aligned}\tag{3.6}$$

For specific values of the coefficients $\tilde{\phi}_a$, the fermion operator has the collective structure of the *s* boson

$$\sum_a \tilde{\phi}_a A_0^\dagger(aa)\rightarrow s^\dagger \tag{3.7}$$

and $|Z\rangle$ is completely equivalent to a purely boson state $|\Phi_B\rangle$

$$|Z\rangle=\sum_i z_i|\Phi_{BF}^i\rangle\leftrightarrow|\Phi_B\rangle,\tag{3.8}$$

where the coefficients z_i are simply related to the structure constants $\tilde{\phi}$. In the same way one finds vectors with the fermion pair coupled to $J_F=2$ which, expressed in the basis $|\Phi_{BF}\rangle$, reconstruct the microscopic structure of the *d* boson

$$\sum_{ab} \tilde{\chi}_{ab}A_{2\mu}^\dagger(ab)\rightarrow d_\mu^\dagger.\tag{3.9}$$

In order to project the spurious states from the model space one has to calculate the values of the coefficients $\tilde{\phi}$ and $\tilde{\chi}$. For one broken pair the spurious states have positive parity, and therefore there will be no spurious states in negative parity bases of our model space.

Various approaches have been used to calculate the values of the coefficients ϕ and χ that define the structure of the operators $S^\dagger$ and $D^\dagger$ [32,33]. The most simple way to determine ϕ and χ is to solve the spherical shell model problem in the space of two particles (or two holes) [34]. Otsuka [35] has used the surface delta interaction (SDI)

$$V_{\rm SDI}(1,2)=4\pi V_0\delta(\vec{r}_1-\vec{r}_2)\,\delta(r_1-R_0)\tag{3.10}$$

in a fermion space of degenerate *j* shells. R_0 is the nuclear radius and the strength V_0 is adjusted to reproduce the energy spacing between the ground state and the state $|2_1^+\rangle$ in semimagic nuclei. The coefficients ϕ and χ are obtained directly from wave functions of the lowest eigenstates of the SDI for a system of two valence nucleons

$$|0_1^+\rangle\approx S^\dagger|\ \rangle,\quad |2_1^+\rangle\approx D^\dagger|\ \rangle.$$

In a more realistic calculation for a specific nucleus, a better approximation would be to use nondegenerate spherical *j* orbitals in a major shell. Another, more sophisticated approach, is based on the broken-pair approximation (Refs. [36,37] and references therein). The structure constants of the operators $S^\dagger$ and $D^\dagger$ are treated as variational parameters in a many-body calculation. The model starts from a shell-model Hamiltonian

$$H=\sum_i \epsilon_i+\sum_{i<j} V_{ij},\tag{3.11}$$

where ϵ_i are single-particle energies and V_{ij} denotes a two-body interaction (for example, a Gaussian phenomenological force). The single-particle energies and the parameters that determine the interaction are obtained from experimental data and model calculations for neighboring nuclei. The variational wave function of the ground-state 0_1^+ in a single closed-shell nucleus is approximated by a condensate of *S* pairs

$$|\Psi_0(\phi)\rangle=N_0(S^\dagger)^p|\ \rangle\simeq|0_1^+\rangle,\tag{3.12}$$

where *p* is the number of valence pairs, N_0 is the normalization constant, and $|\ \rangle$ is the closed-shell core. $S^\dagger$ is defined in (3.4). $|\Psi_0(\phi)\rangle$ is a state of $2p$ particles. The structure coefficients are calculated by minimizing the energy functional

$$\delta\langle\Psi_0(\phi)|H|\Psi_0(\phi)\rangle=0.$$

The first excited state 2_1^+ is assumed to be described by a wave function of $2p$ particles in which one *S* pair is replaced by a *D* pair

$$|\Psi_2(\chi)\rangle=N_2(S^\dagger)^{p-1}D^\dagger|\ \rangle\simeq|2_1^+\rangle.\tag{3.13}$$

Again, by minimizing the energy functional with respect to this variational function, one determines the coefficients χ that define the structure of the correlated D pair. Broken-pair model calculations test whether the coefficients ϕ and χ depend on the number of particles. Namely, an implicit assumption of the IBM is that the microscopic structure of the s and d bosons does not depend on the number of particles in a major shell. In fact, most calculations produce structure coefficients that are approximately constant within a major shell.

With the values of the coefficients ϕ and χ we proceed to construct the spurious states. A problem arises because the correlated S and D pairs are defined in terms of valence nucleons (real fermions) (3.4) and (3.5), while the fermion pairs in our model space correspond to ideal fermions (2.5). Therefore we have to define relations between structure coefficients ϕ and χ, and the coefficients $\tilde{\phi}$ and $\tilde{\chi}$ that appear in definitions (3.7) and (3.9), respectively. The idea is to use again the IBFM mapping (2.12), which relates the nucleon operator $c^\dagger$ and the ideal fermion operator $a^\dagger$. If we take the first three terms in the expansion, the image of the $S^\dagger$ operator acting on the vacuum $|0_B\rangle\otimes|0_F\rangle$ gives

$$\frac{1}{\sqrt{\Omega}}\sum_a \phi_a\alpha_a u_a\sqrt{(2j_a+1)}|s\rangle+\sum_a \phi_a u_a u_a|(j_a j_a)J_F=0\rangle \tag{3.14}$$

and similarly for $D^\dagger$. Other terms in the mapping (2.12) introduce complicated recursion relations for the definition of spurious vectors. We therefore stop at this order of approximation and define the correspondence

$$\tilde{\phi}_a\simeq u_a u_a\phi_a\,,\quad \tilde{\chi}_{ab}\simeq u_a u_b\chi_{ab}\,. \tag{3.15}$$

The projection of the spurious subspace from the model space is now straightforward. For states with given angular momentum and parity J^π, the basis $\mathscr{M}$ can be written as a direct sum of three subspaces

$$\mathscr{M}=\mathscr{B}\oplus\mathscr{F}\oplus\mathscr{G}. \tag{3.16}$$

$\mathscr{B}$ is the boson basis of a system of N bosons

$$\mathscr{B}=\{|\tilde{\phi}_i\rangle, i=1,2,\ldots,n_B\}. \tag{3.17}$$

There are n_B boson states with angular momentum and parity J^π

$$|\tilde{\phi}_i\rangle=|[N](s^{n_s}d^{n_d})^J_\nu;J^\pi\rangle. \tag{3.18}$$

The two subspaces $\mathscr{F}$ and $\mathscr{G}$ contain all states with one broken pair. In $\mathscr{F}$ the two fermions are coupled to angular momenta $J_F=0$ and $J_F=2$

$$\mathscr{F}=\{|\tilde{\phi}_{i+n_B}\rangle, i=1,2,\ldots,n_F\} \tag{3.19}$$

with

$$|\tilde{\phi}_{i+n_B}\rangle=|(j_1j_2)^{J_F=0,2},[N-1](s^{n_s}d^{n_d})^{J_B}_\nu;J^\pi\rangle. \tag{3.20}$$

The subspace $\mathscr{G}$ contains all the remaining states in which the fermions are not coupled to $J_F=0$ or $J_F=2$

$$\mathscr{G}=\{|\tilde{\phi}_{i+n_B+n_F}\rangle, i=1,2,\ldots,n_G\} \tag{3.21}$$

with

$$|\tilde{\phi}_{i+n_B+n_F}\rangle=|(j_1j_2)^{J_F\neq 0,2},[N-1](s^{n_s}d^{n_d})^{J_B}_\nu;J^\pi\rangle. \tag{3.22}$$

All the vectors that we have defined form an orthonormal basis in the model space

$$\mathscr{M}=\{|\tilde{\phi}_i\rangle, i=1,2,\ldots,n_M\}, \tag{3.23}$$

$$\langle\tilde{\phi}_i|\tilde{\phi}_j\rangle=\delta_{ij}\,, \tag{3.24}$$

$$n_M\equiv\dim(\mathscr{M})=n_B+n_F+n_G. \tag{3.25}$$

This decomposition is useful since the spurious states belong to $\mathscr{F}$, and do not have components in the remaining two subspaces. Let us denote the spurious vectors by $|Z_k\rangle$, and assume that there are n_Z of them. An example of a spurious state is given by (3.6). For a linear combination of fermion pair states which reconstructs the microscopic structure of the s or d boson, the number of spurious vectors is equal to the number of states with angular momentum and parity J^π that it can form with all boson states of $(N-1)$ bosons. The spurious states can be expanded in $\mathscr{F}$

$$|Z_k\rangle=\sum_{i=1}^{n_F} z_{ik}|\phi_i\rangle, \tag{3.26}$$

where, for simplicity, a notation is introduced

$$|\phi_i\rangle=|\tilde{\phi}_{i+n_B}\rangle. \tag{3.27}$$

The coefficients z_{ik} are completely determined by the structure constants $\tilde{\phi}_j$ and $\tilde{\chi}_{ij}$. Since they differ in the boson sector, the n_Z spurious vectors are orthogonal (it is also assumed they are normalized), and form a basis of a subspace of $\mathscr{F}$: the spurious subspace

$$\mathscr{Z}=\{|Z_i\rangle, i=1,2,\ldots,n_Z\}. \tag{3.28}$$

Therefore, $\mathscr{F}$ can be further decomposed in a direct sum of the spurious subspace $\mathscr{Z}$ and its orthogonal complement $\tilde{\mathscr{F}}\equiv\mathscr{Z}^\perp$. We write the model space

$$\mathscr{M}=\mathscr{B}\oplus\tilde{\mathscr{F}}\oplus\mathscr{Z}\oplus\mathscr{G}. \tag{3.29}$$

The new model space $\tilde{\mathscr{M}}$, which does not contain spurious states, is the following subspace of $\mathscr{M}$:

$$\tilde{\mathscr{M}}=\mathscr{B}\oplus\tilde{\mathscr{F}}\oplus\mathscr{G}. \tag{3.30}$$

The Hamiltonian matrix has to be constructed and diagonalized in the model space $\tilde{\mathscr{M}}$. We have already defined $\mathscr{B}$, $\mathscr{G}$, and $\mathscr{Z}$. As a last step, a basis $|U_k\rangle$ in $\tilde{\mathscr{F}}$ has to be constructed

$$\tilde{\mathscr{F}}=\{|U_k\rangle, k=1,2,\ldots,n_{\tilde{F}}\}, \tag{3.31}$$

where

$$n_{\tilde{F}}\equiv\dim(\tilde{\mathscr{F}})=n_F-n_Z\,. \tag{3.32}$$

Since they are elements in $\mathscr{F}$, the vectors $|U_k\rangle$ can be expanded

$$|U_k\rangle=\sum_{i=1}^{n_F} u_{ik}|\phi_i\rangle. \tag{3.33}$$

The coefficients are determined from the requirements that $|U_k\rangle$ form an orthonormal basis

$$\langle U_j|U_k\rangle=\delta_{jk}, \tag{3.34}$$

and that they are orthogonal to the subspace of spurious states

$$\langle Z_j|U_k\rangle=0. \tag{3.35}$$

The two conditions can be explicitly written

$$\langle U_k|U_l\rangle=\sum_{i=1}^{n_F}\sum_{j=1}^{n_F} u_{ik}u_{jl}\langle\phi_i|\phi_j\rangle=\sum_{m=1}^{n_F} u_{mk}u_{ml}=\delta_{kl} \tag{3.36}$$

and

$$\langle Z_k|U_l\rangle=\sum_{i=1}^{n_F}\sum_{j=1}^{n_F} z_{ik}u_{jl}\langle\phi_i|\phi_j\rangle=\sum_{m=1}^{n_F} z_{mk}u_{ml}=0, \tag{3.37}$$

or, in the matrix notation

$$U^tU=I, \quad Z^tU=O. \tag{3.38}$$

The system does not have a unique solution. To find a generic solution for the matrix U, a standard Gram-Schmidt orthogonalization procedure for the construction of the basis $|U_k\rangle$ is performed. Finally, the model space $\tilde{\mathscr{M}}$, from which spurious states have been projected, is

$$\tilde{\mathscr{M}}=\{|\tilde{U}_k\rangle,\ k=1,2,\ldots,n_{\tilde{M}}\} \tag{3.39}$$

with

$$n_{\tilde{M}}\equiv\dim(\tilde{\mathscr{M}})=n_M-n_Z=n_B+n_{\tilde{F}}+n_G, \tag{3.40}$$

and the vectors $|\tilde{U}_k\rangle$ are defined

$$\begin{aligned}
|\tilde{U}_k\rangle&\equiv|\tilde{\phi}_k\rangle \quad k=1,2,\ldots,n_B,\\
|\tilde{U}_{k+n_B}\rangle&\equiv|U_k\rangle=\sum_{j=1}^{n_F} u_{jk}|\tilde{\phi}_{j+n_B}\rangle \quad k=1,2,\ldots,n_{\tilde{F}},\\
|\tilde{U}_{k+n_B+n_{\tilde{F}}}\rangle&\equiv|\tilde{\phi}_{k+n_B+n_F}\rangle \quad k=1,2,\ldots,n_G.
\end{aligned} \tag{3.41}$$

TABLE I. Single particle energies ϵ_j, quasiparticle energies E_j, and occupation amplitudes u_j and v_j of neutron levels in ^{116}Sn, used in the calculation with the SDI.

l j	ϵ_j	E_j^{qp}	u_j	v_j
$d_{5/2}$	0.000	2.067	0.311	0.950
$g_{7/2}$	0.838	1.477	0.468	0.884
$s_{1/2}$	1.327	1.268	0.604	0.796
$d_{3/2}$	2.864	1.709	0.922	0.387
$h_{11/2}$	2.561	1.512	0.892	0.453

The matrix of the linear transformation between the old basis in $\mathscr{M}$, and the new basis in $\tilde{\mathscr{M}}$

$$|\tilde{U}_k\rangle=\sum_{j=1}^{n_M} q_{jk}|\tilde{\phi}_j\rangle \quad k=1,2,\ldots,n_{\tilde{M}}, \tag{3.42}$$

has the block-diagonal form

$$Q=\begin{pmatrix} I & O & O\\ O & U & O\\ O & O & I\end{pmatrix} \quad .$$

Q, of course, is not a quadratic matrix since the dimension of $\tilde{\mathscr{M}}$ is smaller than that of $\mathscr{M}$. Finally, the Hamiltonian matrix in $\tilde{\mathscr{M}}$

$$\tilde{H}_{ij}\equiv\langle\tilde{U}_i|H|\tilde{U}_j\rangle,$$

is obtained from the matrix in the old basis

$$H_{ij}\equiv\langle\tilde{\phi}_i|H|\tilde{\phi}_j\rangle,$$

with the transformation

$$\tilde{H}=Q^tHQ. \tag{3.43}$$

IV. A SPHERICAL NUCLEUS – ^{116}Sn

From the structure of the spurious states one expects that they will have a stronger influence on the spectrum of model eigenstates for states of relatively low angular momentum that are found above the yrast line. In this and the following section we use the model to describe the structure of two nuclei. The spherical nucleus ^{116}Sn, in which mostly low spin states are known, and the weakly deformed nucleus ^{82}Sr, where data on bands close to the yrast line extend to $J\approx 20\hbar$.

^{116}Sn is a spherical semimagic nucleus with 16 valence neutrons. The experimental spectrum of low-lying states is almost complete up to $\approx$4.3 MeV [38]. The structure of states has been extensively described in the framework of the broken-pair model [39] and the IBM [40]. The number of bosons is $N=8$. In the model calculations we use two different fermion interactions. In the first case the interaction between valence nucleons is the surface delta interaction (SDI)

$$V_{\rm SDI}(1,2)=4\pi V_0\delta(\vec{r}_1-\vec{r}_2)\,\delta(r_1-R_0).$$

TABLE II. Same parameters as in Table I, but obtained in the broken-pair model, and used in the calculation with the Gaussian fermion interaction.

l j	ϵ_j	E_j^{qp}	u_j	v_j
$d_{5/2}$	0.500	2.199	0.423	0.906
$g_{7/2}$	0.000	2.017	0.378	0.926
$s_{1/2}$	2.000	1.823	0.696	0.717
$d_{3/2}$	2.600	1.792	0.808	0.589
$h_{11/2}$	2.500	1.806	0.922	0.387

TABLE III. Microscopic structure of the s and d bosons in ^{116}Sn, calculated with the SDI fermion interaction. The coefficients ϕ and χ are defined in Sec. III, $\tilde{\phi}_i = u_i u_i \phi_i$ and $\tilde{\chi}_{ij} = u_i u_j \chi_{ij}$. The coefficients are normalized.

$2j_1,2j_2$	1,1	3,3	5,5	7,7	11,11				
ϕ_j	0.175	0.144	0.816	0.456	−0.271				
$\tilde{\phi}_j$	0.224	0.427	0.276	0.349	−0.754				
$2j_1,2j_2$	1,3	1,5	3,3	3,5	3,7	5,5	5,7	7,7	11,11
χ_{ij}	0.074	0.247	0.039	−0.069	0.133	0.920	0.153	0.182	−0.083
$\tilde{\chi}_{ij}$	0.272	0.305	0.219	−0.130	0.379	0.586	0.146	0.262	−0.437

The microscopic structure of the s and d bosons is obtained by diagonalizing the SDI in the valence space of five nondegenerate shells. For the single-particle energies the Kisslinger-Sorensen [41] parametrization is used. The strength $V_0 = -0.22$ MeV is adjusted to reproduce the energy spacing $E(2_1^+) - E(0_1^+) \approx 1.2$ MeV, i.e., it is assumed that the wave function of 0_1^+ has, as the main component, the structure of s bosons, and that 2_1^+ corresponds to the excitation of a d boson. The SDI with a similar strength is used as the residual interaction between fermions in the broken pair. The occupation probabilities and quasiparticle energies are obtained by a standard BCS calculation (without number projection) with Kisslinger-Sorensen single-particle energies and pairing strength $G = 24/A$. The values are given in Table I.

The second fermion interaction is a Gaussian

$$V_{\mathrm{GAUSS}}(1,2) = V_0(\hat{P}_{se} + t\hat{P}_{to}) \exp\{-|\vec{r}_1 - \vec{r}_2|^2/\mu\},$$

where P_{se} and P_{to} are projection operators on singlet-even and triplet-odd states, and t is the mixing parameter. The microscopic structure of bosons has been calculated in the broken-pair model [39]. The single-particle energies are obtained from a BPM calculation of low-lying states in neighboring even-odd nuclei. Their values, together with the corresponding occupation probabilities and quasiparticle energies, are given in Table II. Again, this interaction will consistently be used as the residual interaction between fermions in the broken pair.

In Tables III and IV we display the structure coefficients of the s and d bosons, calculated with the SDI, and the Gaussian interaction in the BPM, respectively.

The parameters of the boson Hamiltonian H_B are adjusted on the lower part of the spectrum (first two states of angular momentum 0^+, 2^+, and 4^+). Their values are $\epsilon = 1.32$, $c_0 = -0.5$, $c_2 = -0.224$, $c_4 = -0.067$, $v_2 = 0.038$, and $v_0 = -0.06$ (all values in MeV). The value of ϵ is actually slightly higher than what one gets from a purely IBM-1 calculation. This adjustment is necessary in order to compensate for the effect of the mixing interaction V_{mix} which, through one broken-pair admixture, lowers in energy these predominantly bosonic states.

To determine the strength of the exchange boson-fermion interaction we performed an IBFM calculation for the low-lying negative parity states in the even-odd neighbor ^{117}Sn [42]. We find that the strength $\Lambda_0 = 0.1$ MeV describes the small energy splitting of the quintuplet of states $[h_{\frac{11}{2}}^- \otimes 2_1^+]^{(J)}$. There is only one type of valence nucleons (neutrons), and therefore the dynamical boson-fermion interaction vanishes. We also find that it is not necessary to include the monopole boson-fermion interaction in the calculation.

For the residual interaction between fermions in the broken pair we use the same fermion interactions that determine the structure of the s and d bosons. The strength of the SDI is adjusted to reproduce the energy spacings between low-lying negative parity states in ^{116}Sn. It turns out that the value $V_0 = -0.2$ MeV is very close to the strength that is used in the construction of the s and d bosons (-0.22 MeV). For the Gaussian interaction we take the same parameters that are used in the calculation of the microscopic structure of the bosons: $V_0 = -35$ MeV (the absolute value cannot be compared with that of the SDI, since the interaction is defined in a different way) and $t = 0.5$ [39].

For the mixing interaction the parameters are $U_2 = 0.13$ MeV for the calculation with the SDI and $U_2 = 0.18$ MeV for the calculation with the Gaussian interaction. In both cases

TABLE IV. Microscopic structure of the s and d bosons in ^{116}Sn, calculated in the broken-pair model with the Gaussian fermion interaction.

$2j_1,2j_2$	1,1	3,3	5,5	7,7	11,11				
ϕ_j	0.161	0.161	0.579	0.766	−0.161				
$\tilde{\phi}_j$	0.323	0.434	0.429	0.452	−0.565				
$2j_1,2j_2$	1,3	1,5	3,3	3,5	3,7	5,5	5,7	7,7	11,11
χ_{ij}	0.231	0.407	0.109	−0.164	0.335	0.409	0.163	0.652	−0.106
$\tilde{\chi}_{ij}$	0.481	0.445	0.265	−0.208	0.379	0.272	0.096	0.345	−0.335

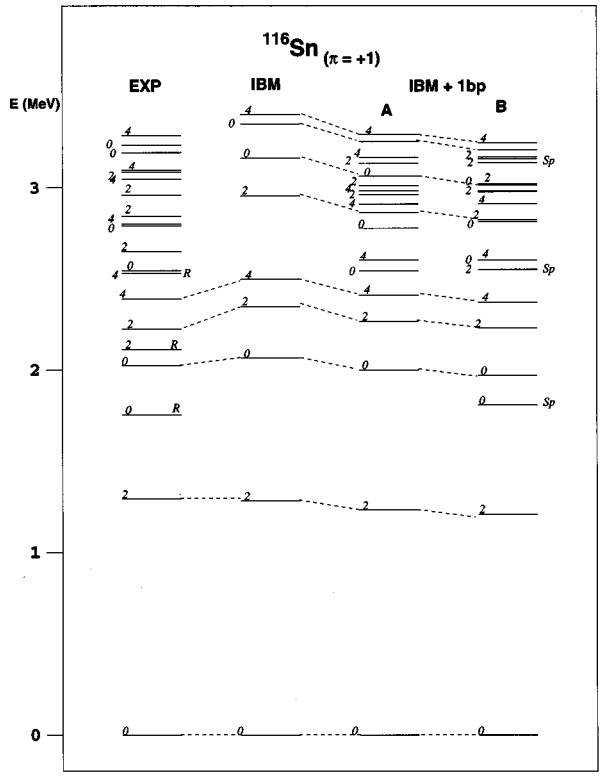

FIG. 1. Positive-parity levels in ^{116}Sn. The figure displays experimental levels and results of model calculation with simple IBM model and IBM+1bp model. The levels in column (B) are calculated without projection of spurious states.

we take $U_0=0$. The main effect of the first term in (2.13) is to lower the positive-parity spectrum with respect to negative-parity states. In the present calculation this is not necessary.

In Fig. 1 the experimental spectrum of positive-parity states is compared with results of model calculation (states up to $\approx$3.3 MeV). The experimental spectrum, in the first column, contains also states that belong to an ''intruder'' rotational band (denoted by R) [43]. These are believed to be predominantly 2p-2h proton states, although objections have been raised about their purely rotational structure [44]. We are not able to simultaneously include proton states in the model space, and therefore the description of the rotational states and their admixture in the neutron vibrational states is beyond the scope of this work. In the second column of Fig. 1 we display the results of a simple IBM-1 calculation. The calculated states are just boson states of the system of 8 bosons, the model space is not extended with broken pairs. The IBM-1 reproduces the excitation energies of low-lying collective states, but the density of calculated states is too low. The third column (A) represents the result of model calculation in the full model space. Spurious states are projected from the bases, and the fermion interaction is the SDI. With the inclusion of explicit fermion degrees of freedom in the broken pair, the density of states above 2 MeV is very close to that observed experimentally. With respect to the pure IBM-1 calculation, the effect of the mixing interaction is to lower states in energy. The wave functions of few lowest states for angular momenta $J=0^+$, 2^+, 4^+, 6^+, and 8^+ are given in Table V. The effect of spurious states is illustrated in the fourth column (B) of Fig. 1. The calculation is performed for the same set of parameters as in column (A), except that here spurious states are not projected from the model space. The dimensions of bases for angular momenta $J=$ 2, 4, 6, 8 are $\approx 10^3$. The number of spurious components in the basis is typically $\leqslant$50. States which are predominantly spurious are denoted by ''Sp.'' In Table VI the percentage of one broken-pair components, and the percentage of spurious components in the wave functions of few lowest states of spin $J=0$, 2, and 4 are given. In the lower part of the spectrum the spurious strength is concentrated in just few states of low spin at intermediate excitation energy, and is negligible in the high spin part of the spectrum. These states with large percentage of spurious components, are completely unphysical and do not have experimental counterparts. Of course, they also mix with other low-lying states and introduce unphysical components in the wave functions. It thus

TABLE V. Main components in the wave functions of positive-parity states in ^{116}Sn, calculated with projection of spurious components. Notation: $|(N)\text{bosons}\rangle=|(s^{n_s}d^{n_d})^J\rangle$ and $|(N-1)\text{bosons}\otimes 1bp\rangle=|(j_1j_2)^{J_F},(s^{n_s}d^{n_d})^{J_B}\rangle$.

$$
\begin{aligned}
|0_1^+\rangle &\simeq 0.9|(s^8)^0\rangle \\
|0_2^+\rangle &\simeq 0.9|(s^6d^2)^0\rangle+0.2|(s^4d^4)^0\rangle \\
|0_3^+\rangle &\simeq -0.9|(\tfrac{1}{2}\tfrac{1}{2})^0,(s^7)^0\rangle-0.2|(\tfrac{11}{2}\tfrac{11}{2})^0,(s^7)^0\rangle \\
|0_4^+\rangle &\simeq 0.2|(\tfrac{1}{2}\tfrac{1}{2})^0,(s^7)^0\rangle-0.8|(\tfrac{7}{2}\tfrac{7}{2})^0,(s^7)^0\rangle-0.3|(\tfrac{11}{2}\tfrac{11}{2})^0,(s^7)^0\rangle \\
|2_1^+\rangle &\simeq 0.9|(s^7d)^2\rangle \\
|2_2^+\rangle &\simeq -0.9|(s^6d^2)^2\rangle-0.2|(s^4d^4)^2\rangle \\
|2_3^+\rangle &\simeq 0.8|(s^5d^3)^2\rangle+0.3|(s^3d^5)^2\rangle \\
|2_4^+\rangle &\simeq -0.8|(\tfrac{7}{2}\tfrac{7}{2})^2,(s^7)^0\rangle-0.4|(\tfrac{11}{2}\tfrac{11}{2})^2,(s^7)^0\rangle \\
|4_1^+\rangle &\simeq 0.9|(s^6d^2)^4\rangle+0.2|(s^4d^4)^4\rangle \\
|4_2^+\rangle &\simeq 0.2|(\tfrac{7}{2}\tfrac{7}{2})^4,(s^7)^0\rangle-0.2|(\tfrac{11}{2}\tfrac{11}{2})^4,(s^7)^0\rangle+0.8|(\tfrac{1}{2}\tfrac{7}{2})^4,(s^7)^0\rangle \\
|4_3^+\rangle &\simeq 0.7|(\tfrac{7}{2}\tfrac{7}{2})^4,(s^7)^0\rangle-0.4|(\tfrac{11}{2}\tfrac{11}{2})^4,(s^7)^0\rangle-0.4|(\tfrac{1}{2}\tfrac{7}{2})^4,(s^7)^0\rangle \\
|6_1^+\rangle &\simeq -0.8|(\tfrac{7}{2}\tfrac{7}{2})^6,(s^7)^0\rangle+0.4|(\tfrac{11}{2}\tfrac{11}{2})^6,(s^7)^0\rangle \\
|6_2^+\rangle &\simeq -0.4|(\tfrac{7}{2}\tfrac{7}{2})^6,(s^7)^0\rangle-0.8|(\tfrac{11}{2}\tfrac{11}{2})^6,(s^7)^0\rangle \\
|6_3^+\rangle &\simeq -0.9|(\tfrac{5}{2}\tfrac{7}{2})^6,(s^7)^0\rangle \\
|8_1^+\rangle &\simeq -0.9|(\tfrac{11}{2}\tfrac{11}{2})^8,(s^7)^0\rangle \\
|8_2^+\rangle &\simeq 0.6|(\tfrac{7}{2}\tfrac{7}{2})^6,(s^6d)^2\rangle-0.6|(\tfrac{11}{2}\tfrac{11}{2})^6,(s^6d)^2\rangle
\end{aligned}
$$

TABLE VI. Percentage of one broken-pair components (first row), and of spurious components (second row) in the wave functions of positive parity states in ^{116}Sn, calculated without projection of spurious vectors.

J_i	0_1	0_2	0_3	0_4	2_1	2_2	2_3	2_4	2_7	4_1	4_2	4_3
% 1bp	0	99	5	99	5	7	98	7	99	8	99	99
% spu	0	87	1	6	1	2	67	1	87	2	0	0

TABLE VII. Collective positive-parity states in ^{116}Sn. The excitation energy of the states (in keV), the percentage of n_d d-boson components, and of one broken-pair components in the wave functions are shown in the table.

J_i	E_x(keV)	n_d=3	n_d=4	n_d=5	n_d=6	n_d=7	n_d=8	1bp
0_5	2886	49	12	10	8	–	–	8
0_6	3041	31	21	–	18	–	16	8
0_8	3254	–	24	–	62	–	–	8
0_{10}	3663	–	11	22	5	38	5	9
2_3	2702	68	–	13	–	–	–	7
2_5	3255	6	30	–	21	8	14	8
2_8	3438	–	26	12	–	31	–	8
2_9	3526	–	7	6	–	–	64	9
2_{12}	3701	–	67	–	11	6	–	9
4_5	3424	7	38	–	23	–	13	9
4_7	3658	–	23	–	–	–	62	9
4_{10}	3795	–	43	5	16	7	9	9

appears that projection of spurious components from the model space is essential for a proper description of excited states with low angular momenta.

In Ref. [38] a number of states in ^{116}Sn were tentatively described as collective IBM states (up to four d bosons). In the present calculation many collective states mix very weakly with broken-pair states, even at rather high excitation energy ($\approx$ 4 MeV). In Table VII we display the wave functions of predominantly collective low-spin states, together with the percentage of one broken-pair admixtures. We note that although the mixing with two-fermion states is weak, the number of d bosons is not a good quantum number, except for few isolated states.

The calculated $B(E2)$ values for transitions between the lowest states are compared with experimental data in Table VIII. The $E2$ transition operator and its parameters are defined in Ref. [19]. For the present calculations, the vibrational charge $e^{\rm vib}=0.84$ is adjusted to reproduce the transition $2_1^+ \rightarrow 0_1^+$, $\chi=0.9$ [45], and the single-particle charge is $e^{\rm sp}=0.5$. The calculated $B(E2)$'s reflect the vibrational structure of the wave functions. The inclusion of two-fermion states does not change the transitions significantly. The $B(E2)$'s actually increase, away from experimental values. The experimental transition probabilities [44], except for $4_1^+ \rightarrow 2_1^+$, are very different from what one would expect for a simple anharmonic vibrator. A possible explanation is the mixing between collective vibrational states and 2p-2h proton rotational states. In Table VIII we include data on transitions from the two "rotational" states 0_{2R}^+ and 2_{2R}^+ to the first excited state 2_1^+. The $B(E2)$'s are large, comparable with values for transitions between collective states. The mixing of 2p-2h proton states with collective neutron states was investigated in Ref. [46]. From the analysis of the wave functions it was suggested that the strong reduction of some $B(E2)$'s with respect to vibrational values, i.e., $0_3^+ \rightarrow 2_1^+$, can be attributed to a destructive interference between rotational and vibrational transition amplitudes. The model space did not include explicit neutron fermion degrees of freedom (broken pairs), and can therefore be regarded as complementary to our calculation. In fact, model calculations did not reproduce excitation energies of low-lying states well.

TABLE VIII. Experimental and calculated $B(E2)$ values (in e^2fm^4) for transitions in ^{116}Sn.

$J_i \rightarrow J_f$	EXP	IBM	IBM+1bp
$2_1^+ \rightarrow 0_1^+$	436	444	485
$0_3^+ \rightarrow 2_1^+$	16	708	757
$0_{2R}^+ \rightarrow 2_1^+$	570	–	–
$2_3^+ \rightarrow 0_3^+$	$\leqslant$67	8	6
$2_3^+ \rightarrow 2_1^+$	168	796	858
$2_{2R}^+ \rightarrow 2_1^+$	134	–	–
$4_1^+ \rightarrow 2_3^+$	$\leqslant$67	2	2
$4_1^+ \rightarrow 2_1^+$	772	766	830

In Fig. 2 we compare the calculated spectrum of positive- and negative-parity states with the experimental data. In the calculation of negative-parity states the same set of parameters is used as for the $\pi=+1$ spectra. Negative-parity states are all based on two-fermion states and, as we have explained earlier, there are no spurious components in $\pi=-1$ bases with only one broken pair. We did not attempt a description of 3^- states. In order to describe their structure, one would probably need p-h excitations of the core [39], or equivalently, an f boson. In the model space generated by valence neutrons only, the first 3^- is approximately 1 MeV higher than the experimental state. This, of course, has also a strong effect on the 5_1^- state through the component $[3^- \otimes 2^+]^{(5)}$. Other negative parity states are in reasonable agreement with experimental data, except for the state 9^-.

In Fig. 3 we compare the positive-parity states calculated using the SDI and the Gaussian fermion interaction. Spurious components are not projected from the bases. Although the two interactions produce different microscopic structures for the s and d bosons (Tables III and IV), the positions of spurious states "Sp" are similar in both cases. The difference in the excitation energies of states that contain sizable broken-pair admixture, derives from different quasiparticle energies used in the two calculations, as well as from different structure of matrix elements of the two fermion interactions.

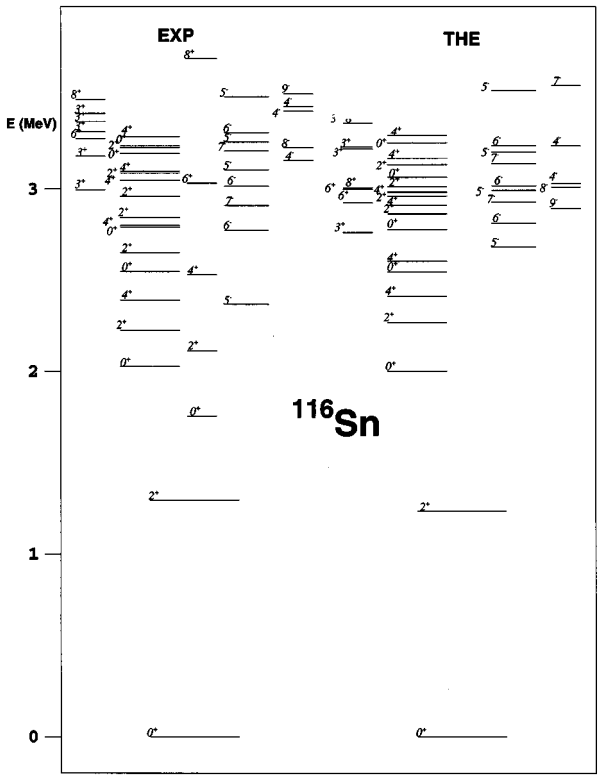

FIG. 2. Comparison between experimental and calculated levels in ^{116}Sn.

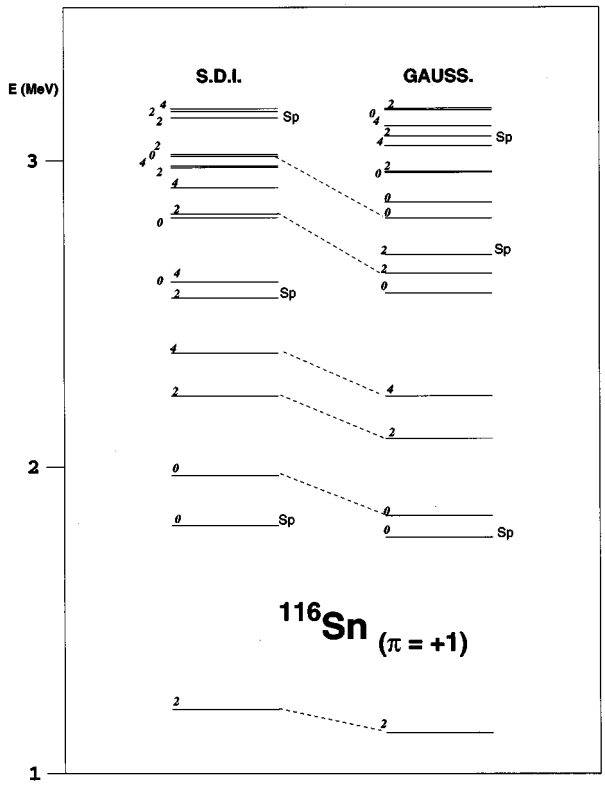

FIG. 3. Positive-parity states in ^{116}Sn, calculated with the SDI and Gaussian fermion interactions. Spurious states are not projected from the model space. Dashed lines connect predominantly collective states, without sizable admixture of one broken pair components.

TABLE IX. Single particle energies ϵ_j, quasiparticle energies E_j, and occupation amplitudes u_j and v_j of proton levels in ^{82}Sr.

lj	ϵ_j	E_j^{qp}	u_j	v_j
$f_{5/2}$	0.170	1.463	0.355	0.935
$p_{3/2}$	0.000	1.594	0.322	0.947
$p_{1/2}$	1.915	1.169	0.882	0.471
$g_{9/2}$	2.862	1.870	0.963	0.270

V. HIGH SPIN STATES- ^{82}Sr

In Refs. [20,23,24] we applied the IBM, extended with the inclusion of one and two broken pairs, to a description of high-spin states in the region of transitional isotopes Sr-Zr. Bands close to the yrast line were compared with experimental data, and moments and transitions for yrast states were calculated. All calculations were performed without projection of spurious states. In this section we apply the model with one broken pair, and projection of spurious components, to ^{82}Sr. There is much recent experimental information on this nucleus [47], and the energy spectrum is very similar to that of ^{84}Zr, a nucleus that we investigated in Ref. [24]. Experimental values of g factors of the 8_2^+ and 10_2^+ states in both ^{82}Sr and ^{84}Sr indicate proton $g_{9/2}$ quasiparticle alignment [48].

The parameters of the boson core Hamiltonian H_B are $\epsilon=0.7$, $c_0=0.2$, $c_2=-0.21$, $c_4=0.14$, $v_2=0.1$, $v_0=-0.2$ (all values in MeV). The number of bosons is $N=8$. The parameters are taken from Ref. [49], where low-spin states in ^{82}Sr are described in IBM-1. The only change is in the parameter ϵ: it has been increased from 0.59 to 0.7. As for ^{116}Sn in the previous section, this is done to compensate for the effects of the mixing interaction in the model space extended by the inclusion of a pair of protons. The fermion model space contains a pair of protons in the major shell 28–50. The single-quasiparticle energies and occupation probabilities (Table IX) are obtained by a BCS calculation using Kissingler-Sorensen [41] single-particle energies and pairing strength $G=23/A$. These single-particle levels are also used in the calculation of the structure coefficients of the s and d bosons. The two-body fermion interaction is the SDI. The strength parameter $V_0=-0.383$ MeV is adjusted to reproduce the excitation energy 1.84 MeV of the state 2_1^+ in the semimagic nucleus ^{88}Sr. The structure coefficients are given in Table X.

TABLE X. Microscopic structure of the s and d bosons in ^{82}Sr, calculated with the SDI fermion interaction. The coefficients ϕ and χ are defined in Sec. III, $\tilde{\phi}_i=u_iu_i\phi_i$ and $\tilde{\chi}_{ij}=u_iu_j\chi_{ij}$. The coefficients are normalized.

$2j_1,2j_2$	1,1	3,3	5,5	9,9		
ϕ_j	0.178	0.635	0.686	−0.307		
$\tilde{\phi}_j$	0.414	0.197	0.258	−0.850		
$2j_1,2j_2$	1,3	1,5	3,3	3,5	5,5	9,9
χ_{ij}	−0.226	0.260	0.614	0.454	0.535	−0.113
$\tilde{\chi}_{ij}$	−0.354	0.448	0.351	0.286	0.371	−0.575

TABLE XI. Dimensions of bases and number of spurious vectors in the basis, for positive-parity states with $J \leqslant 18$ in ^{82}Sr.

J	0	1	2	3	4	5	6	7	8	9	10	11	12	13	14	15	16	17	18
Basis states	175	287	571	595	751	679	723	594	570	427	378	259	216	134	106	57	43	19	14
Spurious states	20	16	48	37	55	40	48	32	34	20	20	10	10	4	4	1	1	0	0

The parameters of the boson-fermion interaction are $\Gamma_0 = 0.35$, $\chi = 0.9$, $\Lambda_0 = 0.6$, and $A_0 = 0$. The parameters of the dynamical interaction are from Ref. [49], where also low spin states in odd-even neighbors of ^{82}Sr are calculated in IBFM. The strength of the exchange interaction is adjusted to reproduce the energy spacings of negative-parity states in ^{82}Sr. It differs considerably from that used for odd-even isotopes [49]. In order to understand the origin of this anomaly, one may consider the coupling of unpaired protons to proton bosons in the ^{82}Sr. To create multiproton states in the even-even nucleus we destroy proton bosons and the effective coupling of the exchange interaction is reduced. In the IBM-2 framework this reduction would be implicit and no adjustment of strength parameters should be needed. However, in our model based on IBM-1, we couple to all the core bosons, irrespective of their nature and the suppression of coupling is greatly diminished. Thus, the need to empirically reduce the strength of coupling parameter. This effect should be especially pronounced near closed shells, and in our case the reduction of the exchange interaction might be due to the subshell closure at $Z = 40$. In any case, the value of the exchange parameter is consistent with values used in our previous calculations for even-even neighbors [20,24]. The parameter of the first term of the mixing interaction, $U_0 = 1.35$ MeV, is adjusted to reproduce the relative position of negative-parity states with respect to the ground state 0_1^+. The strength of the second term, $U_2 = 0.48$ MeV, is chosen in such a way to obtain the correct position ($J = 10$) for the crossing of the collective ground-state band and the lowest two-proton band. The residual interaction between protons in the broken pair is the SDI, with the same strength that is used to construct the microscopic structure of the s and d bosons.

In Table XI, the dimensions of bases for angular momenta $J \leqslant 18$, together with the number of spurious components in each basis, are given. The dimension of the spurious subspace is always small compared to the full model basis.

In Fig. 4 we display the results of model calculation for positive-parity states in ^{82}Sr with protons in broken pairs. Only few lowest levels of each spin are shown in the energy vs angular momentum diagram. The calculated levels are compared with the experimental yrast states. The collective ground-state band is the yrast band up to angular momentum $J = 10^+$. The calculation reproduces the experimental positions of states of the ground-state band, as well as the excitation energies of the first states above the yrast up to spin 8^+. The lowest two proton band starts at 8_3^+, and becomes the yrast band at the state 12_1^+. The calculated states of this band are slightly higher than the corresponding experimental levels, but reproduce the moment of inertia. The main components in the wave functions of the states of this band are $|(\pi g\,\frac{9}{2})^2 J_F = 8, J_B; J = J_F + J_B\rangle$, where $|J_B\rangle$ denotes a collective state of the boson system belonging to the ground-state

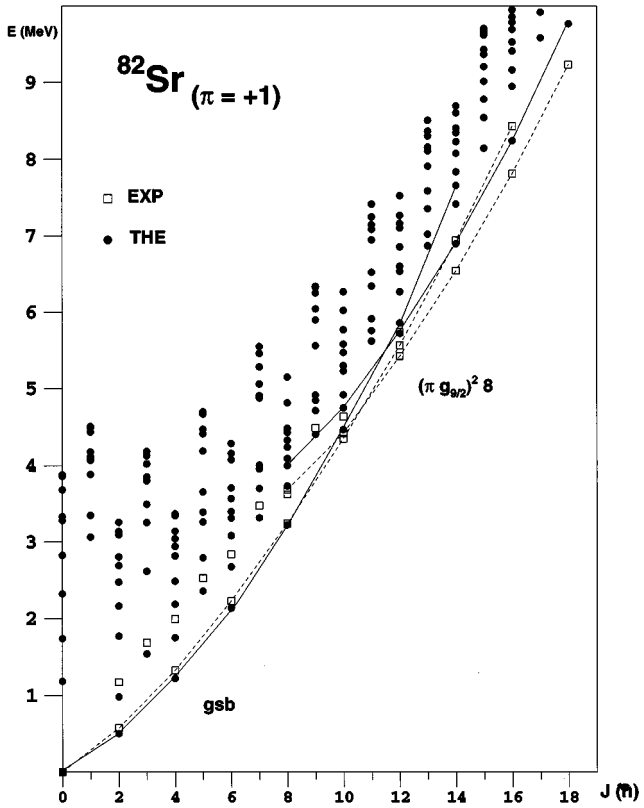

FIG. 4. Energy vs angular momentum diagram for calculated (circles) and experimental (squares) positive-parity states in ^{82}Sr.

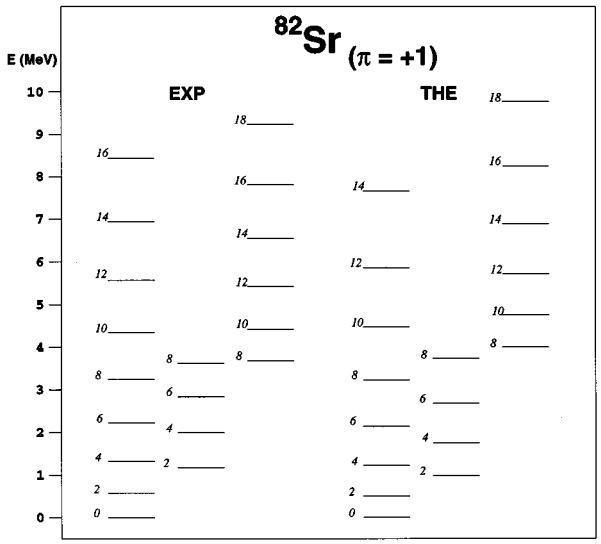

FIG. 5. Comparison between experimental and calculated positive-parity levels in ^{82}Sr.

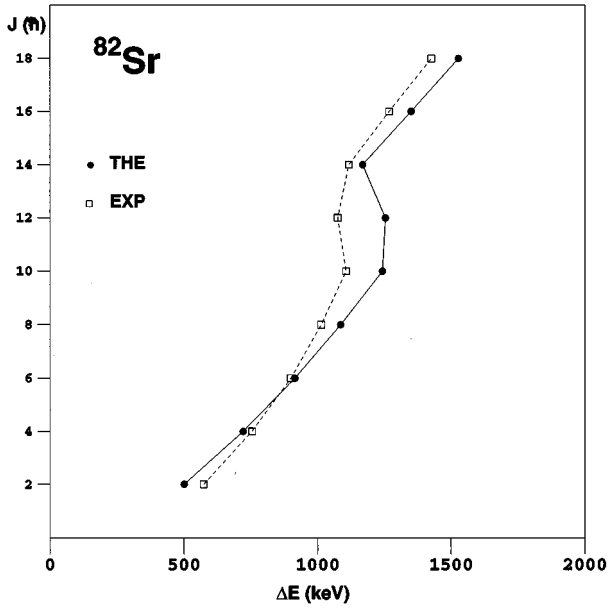

FIG. 6. Angular momentum as a function of transition energy $\Delta E(J)=E(J)-E(J-2)$, for yrast states in ^{82}Sr.

band with angular momentum J_B. The two $g_{9/2}$ protons are completely decoupled from the core and align their angular momenta along the axis of rotation. The fermion angular momentum J_F is a good quantum number for 1bp states close to the yrast line. For states above the yrast line, the Coriolis mixing is much stronger and classification into bands becomes more difficult. In Fig. 5 we compare in a more usual form the lowest calculated levels with experimental data. In Fig. 6 we plot the angular momentum of the yrast states as function of transition energy $E(J)-E(J-2)$. The calculation reproduces the observed weak backbending in the region of band crossing.

Although all calculations are performed with projection of spurious states, it appears that this procedure is not crucial for the description of states close to the yrast line. For a calculation of positive parity states, performed without projection of unphysical components, in Table XII we display the percentage of two-proton components, and the percentage of spurious components in the wave functions of the lowest even-spin states. For states close to yrast, i.e., those seen in the experiment, the spurious components do not exceed 2%. The low-spin states are collective, with very small admixtures of two-fermion states. Only high above the yrast

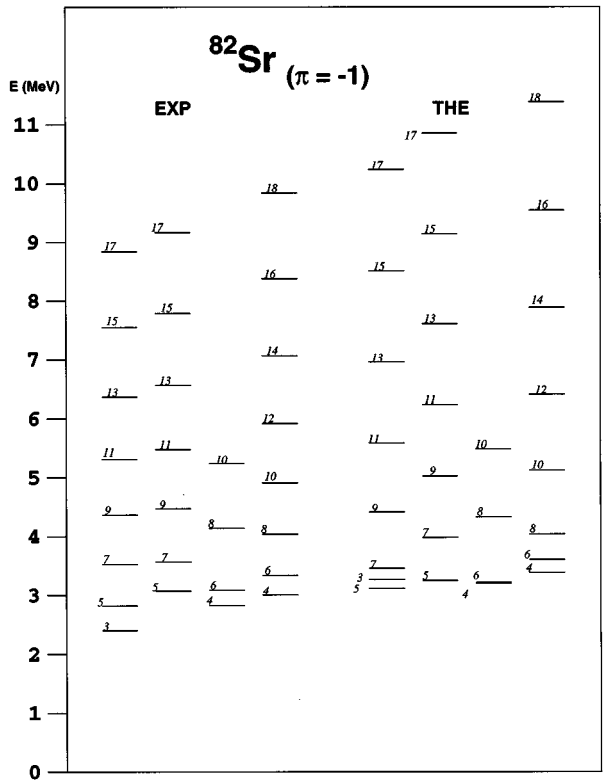

FIG. 7. Experimental negative-parity states in ^{82}Sr compared with results of model calculation.

we find the states 0_5^+ and 2_7^+ which have large spurious components. Except for states which belong to the ground-state band, the high-spin levels ($J>10$) close to the yrast line are one broken-pair states. In the wave functions of these states the main components are based on unique parity fermion orbital ($g_{9/2}$) and total fermion angular momenta $J_F=2j-1=8$ and $J_F=2j-3=6$. On the other hand, spurious states belong to the fermion subspace with fermion angular momenta $J_F=0,2$. This explains the very weak mixing with the spurious subspace for bands of high-spin states at and above the yrast line.

The results for negative parity states are shown in Fig. 7. The mixing of proton orbitals is more pronounced than for positive-parity states, and the wave functions are more complicated. For the lowest states of each angular momentum, the structure of wave functions is predominantly $[f_{5/2}\otimes g_{9/2}]$ coupled to the boson core. The calculated levels reproduce the structure of experimental bands.

TABLE XII. Percentage of one broken-pair components and of spurious components in the wave functions of positive-parity states in ^{82}Sr, calculated without projection of spurious vectors.

J_i	0_1	0_2	0_5	2_1	2_2	2_7	4_1	4_2	6_1	6_2	8_1	8_2	10_1	10_2
% 1bp	15	19	82	18	23	98	19	24	21	24	22	24	23	99
% spu	1	1	54	1	1	57	1	1	1	1	1	1	1	0

J_i	10_3	10_4	12_1	12_2	12_3	12_4	14_1	14_2	14_3	14_4	16_1	16_2	16_3	16_4
% 1bp	23	24	99	23	24	95	100	24	100	26	100	100	26	100
% spu	1	1	0	1	1	0	0	1	0	1	0	0	1	0

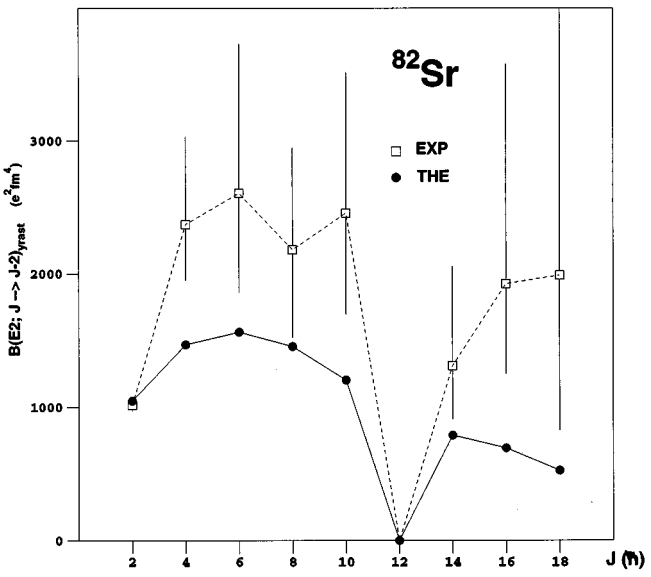

FIG. 8. Experimental (squares) and calculated (circles) $B(E2)$ values for transitions between yrast states in ^{82}Sr.

Finally, in Fig. 8 we compare the calculated $B(E2)$ values for transitions between yrast states with experimental data [47]. The parameters are [19] $e^p=1.1$, $e^{\rm vib}=1.32$, and $\chi=0.9$. The vibrational charge $e^{\rm vib}$ is adjusted to reproduce the transition $2_1^+\rightarrow 0_1^+$. For the parameter χ of the boson quadrupole operator we use the same value as in the dynamical boson-fermion interaction. The calculated $B(E2)$'s are systematically lower than the experimental values, but reproduce the general trend. The decrease of calculated $B(E2)$'s for the highest angular momenta is caused by truncation of the boson model space.

VI. CONCLUSIONS

In this paper we investigated an extension of the interacting boson model to the physics of high-spin states in nuclei. In addition to the structure of low-spin collective states, the model allows the description of states with relatively high angular momentum ($10\hbar\leqslant J\leqslant 30\hbar$) in even-even nuclei, as well as low-spin states that are located high above the yrast line. In order to generate high angular momentum, and/or include explicit fermionic degrees of freedom in low-spin states, one goes beyond the interacting boson approximation and includes selective noncollective fermion states in the model space. This is done through the successive breaking of the correlated S and D pairs (s and d bosons). The physics of high-spin states is described, in the framework of the IBM, in terms of broken pairs. Compared with traditional models based on the cranking approximation, the present approach provides the advantage that all calculations are performed in the laboratory frame, and therefore produce results (excitation energies, electromagnetic properties) that can be directly compared with experimental data.

The model is applied to two nuclei: ^{116}Sn and ^{82}Sr. ^{116}Sn is a spherical nucleus for which mostly data on low-spin states are available. The structure of low-lying states has been previously described in the broken-pair model and the IBM. By extending the collective space with a pair of neutrons, we are able to describe the energy spectrum up to $\approx$3.5 MeV. In particular, the calculation reproduces the density of states above 2 MeV, and the states of negative parity are in reasonable agreement with experimental data. For ^{116}Sn we find that the projection of spurious states from the model space is important for low-spin states. In a calculation without projection of spurious states, several completely unphysical states of angular momentum $J=0$ and 2 (percentage of spurious components $\geqslant$80%), are found between 2 MeV and 3.5 MeV. Smaller admixtures of spurious components are also found in other low-lying states. The distribution of the lowest spurious states does not depend very much on whether the boson structure coefficients are calculated using the SDI or the Gaussian fermion interaction in the BPM. The calculated $B(E2)$ values for transitions between the lowest states reflect the vibrational structure of the wave functions. The experimental data, on the other hand, seem to indicate a rather strong mixing between collective neutron states and the ''intruder'' rotational band based on proton 2p-2h states. The description of this mixing is beyond the scope of our model.

For the weakly deformed nucleus ^{82}Sr there are many recent experimental data on states close to the yrast line. Similar to our previous calculations in this region, the model describes the structure of positive- and negative-parity bands that extend up to 10 MeV excitation energy. Calculations reproduce the observed backbending in the region of band crossing, as well as the general trend in the $B(E2)$ values for transitions along the yrast line. In a calculation of positive parity states, performed without projection of spurious states, we have found a negligible percentage of spurious components in the wave functions of states close to yrast. Results indicate that projection of spurious components is less important for the description of high-spin states. This is encouraging, since the projection procedure necessitates that all valence orbitals are present in the fermion basis, and therefore the full model space becomes prohibitively large for nuclei with many bosons, e.g., deformed nuclei. On the other hand, if the projection procedure is included, the strength of the pair-breaking interaction can be increased without the danger that spurious components become dominant in the wave functions of low-lying states.

[1] F. Iachello and A. Arima, *The Interacting Boson Model* (Cambridge University Press, Cambridge, England, 1987).
[2] A. Arima and F. Iachello, Phys. Rev. Lett. **35**, 10 (1975).
[3] F. Iachello and P. Van Isacker, *The Interacting Boson-Fermion Model* (Cambridge University Press, Cambridge, England, 1991).
[4] A. Gelberg and A. Zemel, Phys. Rev. C **22**, 937 (1980).
[5] I. Morrison, A. Faessler, and C. Lima, Nucl. Phys. **A372**, 13 (1981).

[6] A. Faessler, S. Kuyucak, A. Petrovici, and L. Petersen, Nucl. Phys. **A438**, 78 (1985).
[7] S. Kuyucak, A. Faessler, and M. Wakai, Nucl. Phys. **A420**, 83 (1984).
[8] N. Yoshida, A. Arima, and T. Otsuka, Phys. Lett. **114B**, 86 (1982).
[9] N. Yoshida and A. Arima, Phys. Lett. **164B**, 231 (1985).
[10] C.E. Alonso, J.M. Arias, and M. Lozano, Phys. Lett. B **177**, 130 (1986).
[11] A. Zemel and J. Dobes, Phys. Rev. C **27**, 2311 (1983).
[12] D.S. Chuu and S.T. Hsieh, Phys. Rev. C **38**, 960 (1988).
[13] D.S. Chuu, S.T. Hsieh, and H.C. Chiang, Phys. Rev. C **40**, 382 (1989).
[14] S.T. Hsieh and D.S. Chuu, Phys. Rev. C **43**, 2658 (1991).
[15] S.T. Hsieh, H.C. Chiang, and D.S. Chuu, Phys. Rev. C **46**, 195 (1992).
[16] H.C. Chiang, S.T. Hsieh, and H.Z. Sun, Phys. Rev. C **49**, 1917 (1994).
[17] D. Vretenar, V. Paar, G. Bonsignori, and M. Savoia, Phys. Rev. C **42**, 993 (1990).
[18] F. Iachello and D. Vretenar, Phys. Rev. C **43**, 945 (1991).
[19] D. Vretenar, V. Paar, G. Bonsignori, and M. Savoia, Phys. Rev. C **44**, 223 (1991).
[20] P. Chowdhury *et al.*, Phys. Rev. Lett. **67**, 2950 (1991).
[21] Y. Alhassid and D. Vretenar, Phys. Rev. C **46**, 1334 (1992).
[22] D. Vretenar, G. Bonsignori, and M. Savoia, Phys. Rev. C **47**, 2019 (1993).
[23] C.J. Lister, P. Chowdhury, and D. Vretenar, Nucl. Phys. **A557**, 361c (1993).
[24] A.A. Chisthi, P. Chowdhury, D.J. Blumenthal, P.J. Ennis, C.J. Lister, Ch. Winter, D. Vretenar, G. Bonsignori, and M. Savoia, Phys. Rev. C **48**, 2607 (1993).
[25] G. de Angelis *et al.*, Phys. Rev. C **49**, 2990 (1994).
[26] D. Vretenar, G. Bonsignori, and M. Savoia, Z. Phys. A **351**, 289 (1995).
[27] F. Iachello and O. Scholten, Phys. Rev. Lett. **43**, 679 (1979).
[28] I. Talmi, *Simple Models of Complex Nuclei* (Harwood Academic, New York, 1993).
[29] O. Scholten, ''The Interacting Boson Fermion Model and its Applications,'' PhD thesis, Groningen, 1980.
[30] G. Bonsignori, K. Allaart, and A. Van Egmond, Prog. Part. Nucl. Phys. **9**, 431 (1983).
[31] K. Allaart, G. Bonsignori, M. Savoia, and V. Paar, Nucl. Phys. **A458**, 412 (1986).
[32] T. Otsuka, A. Arima, and F. Iachello, Nucl. Phys. **A309**, 1 (1978).
[33] F. Iachello and I. Talmi, Rev. Mod. Phys. **59**, 339 (1987).
[34] T. Otsuka, A. Arima, F. Iachello, and I. Talmi, Phys. Lett. **76B**, 139 (1978).
[35] T. Otsuka, Phys. Rev. Lett. **46**, 710 (1981).
[36] K. Allaart, E. Boeker, G. Bonsignori, M. Savoia, and Y.K. Gambhir, Phys. Rep. **169**, 210 (1988).
[37] T. Otsuka, T. Mizusaki, and K.H. Kim, in the *Proceedings of International Conference on Perspective for the Interacting Boson Model on Occasion of its 20th Anniversary*, Padova, Italy, 13-17 June 1994, edited by R.F. Casten *et al.* (World Scientific, Singapore, 1994), p. 33.
[38] S. Raman, T.A. Walkiewicz, S. Kahane, E.T. Jurney, J. Sa, Z. Gacsi, J.L. Weil, K. Allaart, G. Bonsignori, and J.F. Shriner, Jr., Phys. Rev. C **43**, 521 (1991).
[39] G. Bonsignori, M. Savoia, K. Allaart, A. Van Egmond, and G. Te Velde, Nucl. Phys. **A432**, 389 (1985).
[40] I. Morrison and R. Smith, Nucl. Phys. **A350**, 89 (1980).
[41] L.S. Kisslinger and R.A. Sorensen, Rev. Mod. Phys. **35**, 853 (1963).
[42] R.L. Auble, Nucl. Data Sheets **25**, 315 (1978).
[43] J. Bron, W.H.A. Hesselink, A. Van Poelgeest, J.J.A. Zalmstra, M.J. Uitzinger, H. Verheul, K. Heyde, M. Waroquier, H.J. Vincx, and P. Van Isaker, Nucl. Phys. **A318**, 335 (1979).
[44] A. Backlin, N.G. Jonsson, R. Julin, J. Kantele, M. Luontama, A. Passoja, and T. Poikolainen, Nucl. Phys. **A351**, 490 (1981).
[45] Y.K. Gambir, P. Ring, and P. Schuck, Phys. Rev. C **25**, 2858 (1982).
[46] G. Wenes, P. Van Isaker, M. Waroquier, K. Heyde, and J. Van Maldeghem, Phys. Rev. C **23**, 2291 (1981).
[47] S.L. Tabor, J. Doring, J.W. Holcomb, G.D. Johns, T.D. Johnson, T.J. Petters, M.A. Riley and P.C. Womble, Phys. Rev. C **49**, 730 (1994).
[48] A.I. Kucharska, J. Billowes, and C.J. Lister, J. Phys. G **15**, 1039 (1989).
[49] D. Bucurescu, G. Cata, D. Cutoiu, G. Costantinescu, M. Ivascu, and N.V. Zamfir, Nucl. Phys. **A401**, 22 (1983).